Influence of Tropospheric Ducting on Microwave Propagation in Short Distances

I. Sirkova[1]and M. Mikhalev[2]

Abstract – **Tropospheric ducting effects are normally considered to be a long-range phenomenon and propagation prediction models used in cells planning and channel characteristics assessment usually do not account for them. In this work it is shown that trapping layers, existing significant percentage of time in certain regions, can affect the expected signal level by shifting the location of the interference maximums in comparison to the propagation under standard troposphere conditions.**

Keywords – **Tropospheric ducts, microwave propagation modeling, parabolic equation.**

I. Introduction

The increasing demand for more services and better quality in the mobile communications poses higher requirements to the propagation prediction models applied in network planning tools. In addition, the UMTS radio network is known to be more sensitive to the propagation environment than is the GSM network [1]. The improvement in coverage and interference assessment/prediction optimizes the base stations planning and decreases the cost of system deployment and exploitation.

This work investigates the influence of tropospheric ducting on microwave propagation in short distances. Ducting effects are normally considered to be a long-range phenomenon, [2], leading to signal enhancement near and beyond the radio horizon. Thus, the classical and even more sophisticated propagation prediction models used in cells planning and channel characteristics assessment usually do not account for tropospheric super refraction and ducting. But, as reported in [3], ducts can affect the propagation in short ranges in two ways: they provoke a shift of the location of the last interference maximum (in terms of path loss) and decrease of the signal level near the last interference minimum. In this work calculations of path loss versus range for some common cases of surface-based ducts are compared to the path loss obtained assuming standard troposphere. The calculations are performed using the parabolic equation (PE) method in conjunction with a finite element based numerical scheme [4].

[1]I. Sirkova is with the Institute of electronics, Bulgarian Academy of Sciences, blvd. "Tzarigradsko chaussee" 72, 1784 Sofia, Bulgaria, E-mail: irina@ie.bas.bg

[2]M. Mikhalev is with the Institute of electronics, Bulgarian Academy of Sciences, blvd. "Tzarigradsko chaussee" 72, 1784 Sofia, Bulgaria, E-mail: matam@ie.bas.bg

II. Method Description

The PE approximation to the wave equation and its application to the tropospheric propagation problems are well documented [5-7] and here only brief description of the method is given.

As paraxial approximation, PE assumes the problem has some preferred propagation direction, say, the x-axis in a Cartesian coordinate system, and transforms the scalar wave equation in a 3D PE:

$$\frac{\partial u(x,y,z)}{\partial x} = \frac{i}{2k}\left(\frac{\partial^2 u(x,y,z)}{\partial z^2} + \frac{\partial^2 u(x,y,z)}{\partial z^2}\right) + \frac{ik}{2}\left(n^2(x,y,z)-1\right)t(x,y,z)\,, \quad (1)$$

where k is the free-space wave number, n is the refractive index of the troposphere, $u(x,y,z)$ is the reduced function, [6], related to a field component E as $E(x,y,z) = u(x,y,z)exp(ikx)$. Equation (1) accounts only for forward propagating field and is very accurate at angles within 15° of the direction of x-axis, [8].

The advantage of equation (1) is that it can be easily marched in range: the solution at range $x + \triangle x$ is obtained from that in range x, provided the field is known on an initial plane and adequate boundary conditions on the outer boundaries of the integration domain are given. To solve (1) a finite-element based numerical scheme allowing easier boundary conditions implementation, [7], is used. Due to its simplicity, the 2D form of (1) is the most widely used and has been adopted here.

III. Results and Discussion

In order to point out the influence of the ducting all other propagation mechanisms are ignored and a smooth perfectly conducting underlying surface is assumed. Horizontally polarized Gaussian beam antenna with 2 GHz frequency is used. Studied are different surface-based ducts and positions of the transmitting antenna in respect of the trapping layer. Piece-wise linear range independent profiles for the modified refractivity $M(z)$ ($M(z) = 10^6(m(z)-1), m = n + z/a_e$, where a_e is the Earth radius) are used with small, moderate and strong M-deficits. Results for path loss calculations are compared to those, obtained for standard troposphere conditions. Standard troposphere is characterized by a modified refractivity gradient that increases monotonically at a rate of 0.118 M-units per m.

Fig. 1 shows path loss for h_t=20 m, h_r=10 m, beam-width=2° (without tilt), the red curve a) referring to a surface-based duct with thickness Z_d=50 m and M-deficit $\triangle M$=10 M-units; the black curve b) is for standard troposphere conditions. Fig. 2 shows path loss for the same antennas heights but for beamwidth=4° (without tilt), Z_d=100 m and $\triangle M$=30 M-units. On Fig. 3 are shown the results for a 70 m surface-based duct formed by a trapping layer between h=50 m and h=70 m with $\triangle M$=30 M-units, h_r=10 m, beam-width=4° (without tilt) and different h_t: a) h_t=20 m (the curves are shifted of -30 dB from their real position); b) h_t=30 m; c) h_t=50 m (the curves are shifted of +30 dB); d) h_t=60 m (the curves are shifted of +60 dB). Fig. 4 reports

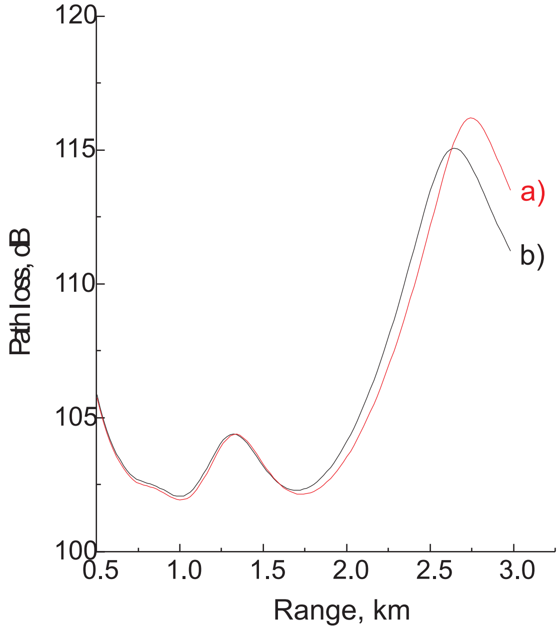

Fig. 1. Path loss for 50 m surface based duct (red curve) and for standard troposphere (black curve), beamwidth=2°, h_t=20 m, h_r=10 m.

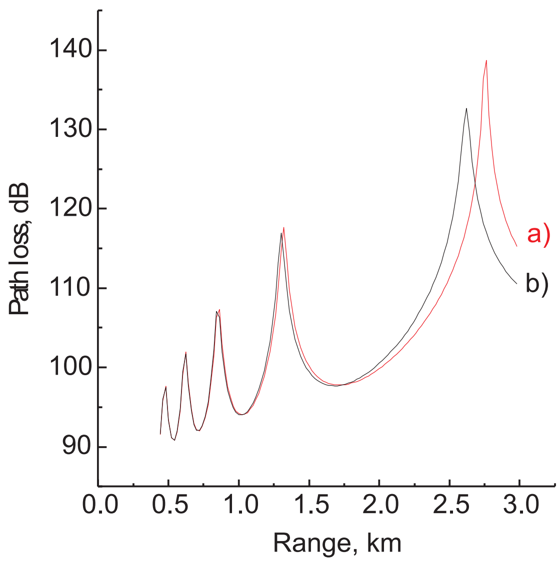

Fig. 2. Path loss for 100 m surface based duct (red curve) and for standard troposphere (black curve), beamwidth=4°, h_t=20 m, h_r=10 m.

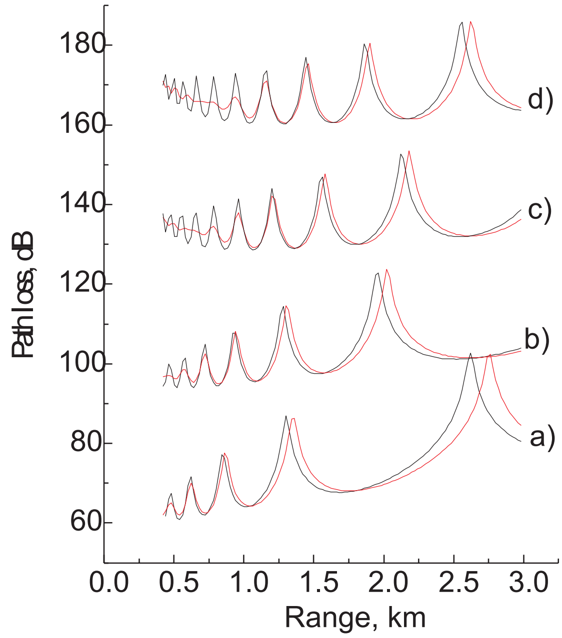

Fig. 3. Path loss for 70 m surface based duct (red curves) and for standard troposphere (black curves), for beamwidth=4°, h_r=10 m and: a) h_t=20 m, b) h_t=30 m, c) h_t=50 m, d) h_t=60 m.

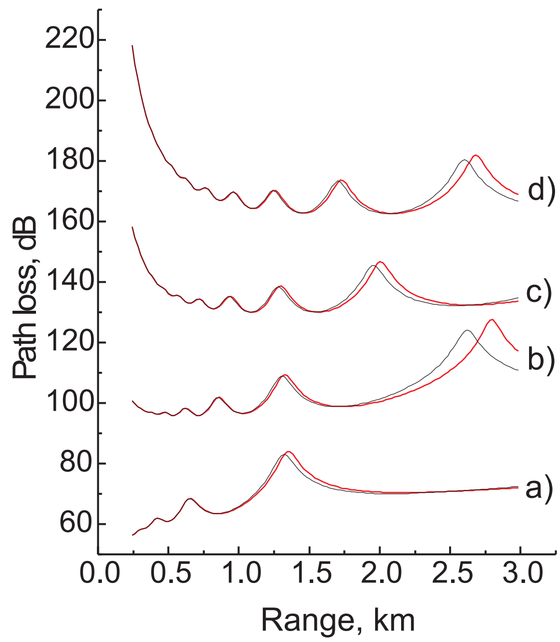

Fig. 4. Path loss for 25 m surface-based duct (red curves) and for standard troposphere (black curves), for beamwidth=2°, h_r=10 m and: a) h_t=10 m, b) h_t=20 m, c) h_t=30 m, d) h_t=40 m.

the results for 25 m surface-based duct ($\triangle M$=10 M-units), h_r=10 m, beam-width=20 (without tilt) and: a) h_t=10 m (shift of -30 dB); b) h_t=20 m, c) h_t=30 m (shift of +30 dB); d) h_t=60 m (shift of +60 dB). The red curves in Figs. 3 and 4 indicate path loss under ducting, the black curves – under standard tropospheric conditions.

From Figs. 1 to 4 it is clearly seen that there is a shift of the location not only of the last interference maximum. As an illustration, in Tables 1 and 2 are given the locations of the path loss (PL) maximums, their values and the differences in dB for these locations between the cases with duct and the standard troposphere. Table 1 refers to the right maximums of Figs. 1 and 2, Table 2 is for the curves d) from Fig. 3 (starting from the right). The shift of the maximums locations is up to 140 m and 100 m for Figs. 1 and 2, respectively. The shifts for Fig. 3 are of 60, 40 and 20 m respectively. There is significant difference in path loss (the column △, dB in the Tables) for one and the same place under ducting and under standard troposphere conditions.

Table 1. Path loss maximums and their locations for Figs. 1 and 2

		PL_{max}, dB	Distance, km	' , dB
Fig. 1	Duct	138.68	2.762	21.62
	Standard trop.	132.64	2.622	14.94
Fig. 2	Duct	116.19	2.742	1.76
	Standard trop.	115.07	2.642	0.19

Table 2. Path loss maximums and their locations for curves d) from Fig. 3

		PL_{max}, dB	Distance, dn	' , dB
Duct	1st max	125.97	2.622	10.96
	2nd max	120.52	1.902	6.76
	3rd max	115.38	1.462	2.06
Standard trop. .	1st max	125.74	2.562	10.45
	2nd max	120.36	1.862	7.19
	3rd max	117.01	1.442	2.81

The decrease of the signal level near the interference minimums has also been investigated. As it is seen from the reported Figures, for the studied cases it is negligible (less than 1 dB).

As far as ducting is known to be present about 15% of the time all over the world [3], and even more often in maritime environment, the duct effects inclusion in radio propagation modeling could improve the coverage and interference prediction.

References

[1] M. Coinchon, A. Salovaara and J. Wagen, ”The impact of radio propagation predictions on urban UMTS planning”, *COST 273 TD(01)041*, Bologna, Italy, 15-17 Oct. 2001.

[2] H. V. Hitney, J. H. Richter, R. A. Pappert, K. D. Anderson and G. B. Baumgartner, Jr., ”Tropospheric radio propagation assessment”, *Proc. IEEE*, vol. 73, pp. 265-283, 1985.

[3] K. D. Anderson, ”Radar detection of low-altitude targets in a maritime environment”, *IEEE Trans. Antennas Propagat.*, vol. 43, no. 6, pp. 609-613, 1995.

[4] I. Sirkova and H. E. Hernandez-Figueroa, ”Local transparent boundary condition applied to the modeling of tropospheric ducting propagation”, *J. Microw. Opt. Technol. Lett.*, vol. 21, no. 5, pp. 343-346, 1999.

[5] J. R. Kuttler and G. D. Dockery, ”Theoretical description of the parabolic approximation/Fourier split-step method of representing electromagnetic propagation in the troposphere”, *Radio Sci.*, vol. 26, pp. 381-393, 1991.

[6] K. G. Craig and M. F. Levy, ”Parabolic equation modeling of the effects of multipath and ducting on radar systems”, *IEE Proc.-F*, vol. 138, pp. 153-162, 1991.

[7] I. Sirkova, ”On transparent boundary conditions application to the tropospheric ducting propagation modeling”, *J. Applied Electromagnetism*, vol. 3, no. 1, pp. 59-78, 2000.

[8] Ch. Zelley and C. Constantinou, ”A 3-dimensional parabolic equation applied to the VHF/UHF propagation over irregular terrain”, *IEEE Trans. Antennas Propagat.*, vol. AP-47, no. 10, pp. 1586-1596, 1999.